



**HAL**  
open science

## The biomechanical model of the long finger extensor mechanism and its parametric identification

Anton Dogadov, Mazen Alamir, Christine Serviere, Franck Quaine

► **To cite this version:**

Anton Dogadov, Mazen Alamir, Christine Serviere, Franck Quaine. The biomechanical model of the long finger extensor mechanism and its parametric identification. *Journal of Biomechanics*, 2017, 58, pp.232-236. 10.1016/j.jbiomech.2017.04.030 . hal-01583110

**HAL Id: hal-01583110**

**<https://hal.science/hal-01583110>**

Submitted on 6 Sep 2017

**HAL** is a multi-disciplinary open access archive for the deposit and dissemination of scientific research documents, whether they are published or not. The documents may come from teaching and research institutions in France or abroad, or from public or private research centers.

L'archive ouverte pluridisciplinaire **HAL**, est destinée au dépôt et à la diffusion de documents scientifiques de niveau recherche, publiés ou non, émanant des établissements d'enseignement et de recherche français ou étrangers, des laboratoires publics ou privés.

# The Biomechanical Model of the Long Finger Extensor Mechanism and its Parametric Identification

Anton Dogadov, Mazen Alamir, Christine Serviere, Franck Quaine

Univ. Grenoble Alpes, GIPSA-Lab, F-38000 Grenoble, France

CNRS, GIPSA-Lab, F-38000 Grenoble, France

**Abstract** – The extensor mechanism of the finger is a structure transmitting the forces from several muscles to the finger joints. Force transmission in the extensor mechanism is usually modeled by equations with constant coefficients which are determined experimentally only for finger extension posture. However, the coefficient values change with finger flexion because of the extensor mechanism deformation. This induces inaccurate results for any other finger postures. We proposed a biomechanical model of the extensor mechanism represented as elastic strings. The model includes the main tendons and ligaments. The parametric identification of the model in extension posture was performed to match the distribution of the forces among the tendons to experimental data. The parametrized model was used to simulate three degrees of flexion. Furthermore, the ability of the model to reproduce how the force distribution in simulated extensor mechanism changes according to the muscle forces was also demonstrated. The proposed model could be used to simulate the extensor mechanism for any physiological finger posture for which the coefficients involved in the equations are unknown.

**Keywords** – biomechanical modelling, finger modelling, extensor mechanism, tendons

1  
2  
3  
4  
5  
6  
7  
8  
9  
10  
11  
12  
13  
14  
15  
16  
17  
18  
19  
20  
21  
22  
23  
24  
25  
26

## INTRODUCTION

The extensor mechanism (EM) of the finger (the extensor apparatus, extensor expansion, extensor assembly, dorsal aponeurosis, etc.) is a complex anatomical structure which transmits the forces of several extrinsic and intrinsic hand muscles to the finger joints (See Fig. 1a,b in the Method section). It is situated on the dorsal surface of the finger bones and is involved in both extension and flexion of the finger joints.

Owing to its important role in force transmission, the EM has been incorporated into biomechanical models of the finger (Sancho-Bru *et al.*, 2001; Vigouroux *et al.*, 2007; Hu *et al.*, 2014). For the extended posture it is usually modeled by an equation system proposed by Chao *et al.* (1989) which represents the internal-force distribution in the tendon network (see eq. 3). To take into account the EM for other postures it is usually represented as a 3D-network of extensible or non-extensible strings placed on finger bones at given joint angles. Some models of this type may include only tendons as the individual elements (Giurintano and Sancho, 1999; Valero-Cuevas and Lipson, 2004; Hu *et al.*, 2014). Some models also take ligaments into account as separated elements or incorporate them into a model as constraints (Leijnse and Spoor, 2012; Sachdeva *et al.*, 2015; Vaz *et al.*, 2015). The models may contain a high number of elements, which allows modeling of the EM with a high degree of precision in order to simulate the clinical deformities of the mechanism (Sachdeva *et al.*, 2015). However, such 3D-models contain many unknown parameters that should be determined. It seems that most studies in this field have only focused on EM modelling but not on its parametrization and validation.

The purpose of this study was to create a numeric model of the long finger EM that includes main tendons and ligaments as well as to perform a parametric identification of the model to match the force distribution given by Chao equation system for the extension posture (4). The proposed model of the EM with the parametrization algorithm aims to contribute to improving the relevance of biomechanical models of finger in simulating all feasible posture given in the literature for normal finger (Leijnse *et al.*, 2010).

28 **Model**

29 The EM was modeled as a network of elastic bands. Fig. 1c shows the components of the  
 30 EM included in the model. Each EM component, or band, was discretized by the chain of the  
 31 points, connected by elastic elements. Hence, the EM position was represented by the array  $\mathbf{x}$  of  
 32 x,y,z-coordinates of points forming the EM. Each two sequential points, discretizing an EM  
 33 band, were connected by a spring with a linear elasticity model. The bones were modeled by  
 34 cylinders and spheres and completed by three auxiliary cylinders, perpendicular to the bones (*a*,  
 35 *b*, *c* in Fig. 1c), which replace the function of pulleys or condyles.

36 The forces of dorsal ulnar interosseous *ui*, extensor digitorum *ed*, dorsal radial  
 37 interosseous *ri*, and lumbrical *lu* muscle were used as the external ones. The fraction of these  
 38 forces applied to EM will be henceforth denoted as  $\Phi = [\alpha_{ui}\Phi_{ui} \ \alpha_{ed}\Phi_{ed} \ \alpha_{ri}\Phi_{ri} \ \alpha_{lu}\Phi_{lu}]^T$ . The  
 39 muscle forces  $\Phi_j$  ranged from 2.45-7.35 N and were taken from the cadaveric studies by Garcia-  
 40 Elias *et al.* (1991) and by Hurlbut *et al.* (1995). The weight coefficients  
 41  $\alpha = [0.626 \ 0.500 \ 0.267 \ 1.00]^T$  were used to take into account the fact that there is a fraction of  
 42 *ui*, *ed* and *ri*-muscle force that is applied to the base of metacarpal bone and is not transmitted by  
 43 the tendons of the EM (Eyler and Markee, 1954; Zancolli, 1979). Their values were estimated  
 44 from Chao *et al.* (1989).

45 The principle of Minimum Potential Energy was used to find the equilibrium state, in  
 46 which the EM internal forces balance the muscle forces. At iteration  $k+1$  the potential energy  
 47 (*PE*) of the EM was calculated as a sum of the strain energy (*SE*) of the spring system and work  
 48 potential of the muscle forces (*WP*):

$$PE(\mathbf{x}_{k+1}) = SE(\mathbf{x}_{k+1}) + WP(\mathbf{x}_{k+1}, \mathbf{x}_k, \Phi) + g(\mathbf{x}_{k+1}), \quad (1)$$

49 where *g* represents penalty term, which was added to enforce the constraint expressing the fact  
 50 that the points forming EM should not penetrate the bone surface.

51 The Broyden–Fletcher–Goldfarb–Shanno method (BFGS) was used to find the minimum of  
 52 potential energy. The array  $\mathbf{x}$  at iteration  $k+1$  was calculated as:

$$\mathbf{x}_{k+1} = \mathbf{x}_k - \mathbf{H}_k \cdot \nabla PE, \quad (2)$$

53 where  $\mathbf{H}$  is a BFGS approximation to the Hessian matrix.

#### 54 **Parametrization**

55 The distribution of the forces among the EM tendons can be described by the equation  
 56 system, proposed by Chao *et al.* (1989):

$$\begin{cases} F_{te} = C_1 F_{ub} + C_2 F_{rb} \\ F_{rb} = C_3 \Phi_{ed} + C_4 \Phi_{ri} + C_5 \Phi_{lu} \\ F_{ub} = C_6 \Phi_{ui} + C_7 \Phi_{ed} \\ F_{me} = C_8 \Phi_{ui} + C_9 \Phi_{ed} + C_{10} \Phi_{ri} + C_{11} \Phi_{lu} \end{cases}, \quad (3)$$

57 where  $F_i$  are the internal forces in the tendons,  $\Phi_i$  are the muscle forces applied to the EM. The  
 58 internal force subscripts are abbreviations of tendon names, listed in Table 1. The coefficients  
 59  $C_1 \dots C_{11}$  will be further denoted as a vector  $\mathbf{C} = [C_1 \dots C_{11}]^T$ , which determine the force  
 60 distribution among the bands of the EM. The values of  $\mathbf{C}$  depend on the properties of the tendons  
 61 and the angles between them. These values were measured for the extended posture (Chao *et al.*  
 62 1989):

$$\begin{cases} F_{te} = 1.000 F_{ub} + 1.000 F_{rb} \\ F_{rb} = 0.167 \Phi_{ed} + 0.133 \Phi_{ri} + 0.667 \Phi_{lu} \\ F_{ub} = 0.313 \Phi_{ui} + 0.167 \Phi_{ed} \\ F_{me} = 0.313 \Phi_{ui} + 0.167 \Phi_{ed} + 0.133 \Phi_{ri} + 0.333 \Phi_{lu} \end{cases} \quad (4)$$

63 The experimentally defined coefficients in (4) will be denoted as a vector  $\hat{\mathbf{C}} = [1.00 \dots 0.33]^T$ .

64 For each simulation, the coefficients, describing the force distribution in simulated EM  
 65 were estimated and denoted as  $\mathbf{C}^* = [C_1^* \dots C_{11}^*]^T$ . There are more unknown coefficients than  
 66 equations in (3). Hence, to determine  $\mathbf{C}^*$  the EM should be simulated for different muscle force

67 sets, which increases the number of equations in (3). The forces from the right part of (3) after  
 68 equation number increase were denoted as the matrix  $\mathbf{B}^*$ , and the forces from the left part were  
 69 denoted as the matrix-column  $\mathbf{A}^*$ . As  $\mathbf{A}^*$  was calculated to be accurate within a certain degree of  
 70 error, the values of the coefficients were estimated by Tikhonov regularization and were denoted  
 71  $\mathbf{C}^*$ :

$$\mathbf{C}^* = \arg \min_{\mathbf{C}} \left( \|\mathbf{B}^* \mathbf{C} - \mathbf{A}^*\|^2 + \alpha \|\mathbf{C}\|^2 \right), \quad (5)$$

72 where a regularization parameter  $\alpha$  was set to 0.01.

73 It should be noted, that the muscle force sets, applied to the model to estimate  $\mathbf{C}^*$ , should  
 74 be relatively close, otherwise it can modify the EM configuration and bias  $\mathbf{C}^*$ . The study of the  
 75 muscle force value effect on  $\mathbf{C}^*$  is described in the next subsection.

76 A model parametrization was performed to make the model-describing coefficients  $\mathbf{C}^*$  fit  
 77 the experimentally measured coefficients  $\hat{\mathbf{C}}$ . The lengths of two intercrossing bands, extensor  
 78 lateral band *el* and interosseous medial band *im* (2 and 5 in Fig. 1) were chosen as the identified  
 79 parameters, denoted by a vector  $\mathbf{l} = [l_{el} \ l_{im}]^T$ . These tendons were chosen, because they have a  
 80 strong influence on the EM configuration (Schultz *et al.*, 1981). The root-mean-square error  
 81 between  $\mathbf{C}^*$  and  $\hat{\mathbf{C}}$  was used as a cost-function  $J(\mathbf{l})$ ,

$$J(\mathbf{l}) = \sqrt{\frac{\sum_{q=1}^Q (\hat{C}_q(\mathbf{l}) - C_q^*(\mathbf{l}))^2}{Q}} \quad (6)$$

82 where  $Q$  denotes the number of coefficients ( $Q=11$ ).

83 The Nelder-Mead algorithm (`fminsearch` function in Matlab R2012b, MathWorks,  
 84 Natwick, MA) was used to solve the unconstrained problem of  $J(\mathbf{l})$  minimization.

$$\mathbf{l}_{opt} = \arg \min_{\mathbf{l}} J(\mathbf{l}), \quad (7)$$

85 The starting point of the algorithm corresponded to such EM configuration, in which all lateral  
86 and medial bands were tight (2 and 3, 4 and 5 in Fig. 1).

### 87 **Sensitivity analysis**

88 After the model was parametrized, the sensitivity analysis was performed for the fully  
89 extended posture. As the EM is deformable, the force distribution among the tendons could vary  
90 when the muscle forces change. For the EM model this distribution is represented by  $\mathbf{C}^*$ . The  
91 sensitivity of  $\mathbf{C}^*$  to the variation in muscle force values, which are the model inputs, was  
92 calculated as:

$$SI(C_q^*)_j = \frac{C_q^*(\Phi_1, \dots, \Phi_j + \Delta\Phi_j, \dots, \Phi_n) - C_q^*(\Phi_1, \dots, \Phi_j - \Delta\Phi_j, \dots, \Phi_n)}{2\Delta\Phi_j}, \quad (8)$$

93 where  $\Delta\Phi_j$  was 0.5 N. The positive value of a sensitivity index  $SI(C_q^*)_l$  indicates that  $q$ -th  
94 coefficient increases when the force of  $j$ -th muscle increases.

## 95 **RESULTS**

96 The results address first the parametrization and the simulation of different postures using  
97 the parametrized model and, finally, the sensitivity analysis. Moreover, we used the parametrized  
98 model to estimate the coefficients  $\mathbf{C}^*$  for a sequence of physiological postures (Harris and  
99 Rutledge, 1972). These coefficients are presented as a supplementary material for this paper.  
100 Their values need to be interpreted with caution as they strongly depend on MCP, PIP, and DIP  
101 joint angles (Wook *et al.*, 2008), and there may be a lot of feasible combinations of these angles  
102 (Leijnse *et al.*, 2010). Hence, given coefficients can be used for the investigated postures;  
103 otherwise the coefficients should be recalculated accordingly to the proposed method.

### 104 **Parametrization**

105 The identified tendon lengths for  $l_{el}$  and  $l_{im}$  are given in Table 2. The identified value of  
106  $l_{im}$  is 10% lower than the value defined by anatomical survey (Table 1). No comparison was  
107 possible for  $l_{el}$  as no published data exists. The identified parameters results in a very good fit for

108  $C_1^*$ ,  $C_2^*$ ,  $C_6^*$ , and  $C_8^*$  (Fig. 2). Coefficients  $C_1^*$ , and  $C_2^*$  represent the fraction of the force in  
109 ulnar and radial lateral band  $rb$  and  $ub$  (9 in Fig. 1) transmitted to terminal extensor tendon  $te$  (10  
110 in Fig. 1).  $C_6^*$  and  $C_8^*$  represent the fraction of the  $ui$ -muscle transmitted to  $ub$  and medial  
111 extensor tendon  $me$  (6 in Fig.1). The major difference concerns coefficients  $C_5^*$ , and  $C_{11}^*$ ,  
112 related to the fraction of  $lu$ -muscle transmitted to  $rb$  and  $me$ -tendon.

113 The identified parameter set was used to model three degrees of extension observed in  
114 (Garcia-Elias *et al.*, 1991; Hurlbut and Adams, 1995), which are full flexion, mid-flexion and  
115 full extension. The simulation results are shown in Fig. 3. The changes of the EM configuration  
116 with extension can be seen from the figure Fig. 3. The extensor hood shifts proximally (1 in  
117 Fig. 3b) while  $ub$  and  $rb$ -tendon shift medially (9 in Fig. 3b). The retention apparatus is also  
118 affected by changes: the retinacular ligament (7 in Fig. 3d, e) becomes tight and triangular  
119 ligament (8 in Fig. 3d, e) relaxes with extension.

## 120 Sensitivity analysis

121 Fig. 4 represents sensitivity indices  $SI(C_q^*)_j$ , which show how the values of  $C^*$  change  
122 with respect to muscle force variation. It can be seen that the most significant changes are  
123 observed for  $C_3^*$ ,  $C_4^*$ , and  $C_5^*$ , which correspond to fractions of  $ed$ ,  $ri$ , and  $lu$ -muscle forces  
124 transmitted to  $rb$ -tendon.

## 125 DISCUSSION

126 In this study, a biomechanical model of the EM was proposed to simulate the changes in  
127 the EM configuration with posture in order to better understand force transmission in the bands  
128 and thus accurately model the finger biomechanics behavior. The model was inspired by the  
129 model proposed by Valero-Cuevas and Lipson (2004). The EM was represented as a network of  
130 strings to simulate the change in configuration according to different postures. One improvement  
131 lies in the inclusion of the triangular and oblique retinacular ligaments in the model.

132           The parametrization of the model was firstly performed to fit the distribution of the forces  
133 among the tendons to experimental data for the fully extended posture. Finally, we calculated the  
134 sensitivity of the parametrized model to the variation of the muscle force values.

### 135 **Parametrization**

136           The parametric identification of the model was performed to make the coefficients  
137 describing the model fit the values given by Chao *et al.* (1989). The more important  
138 discrepancies between the simulations and the measurements concern the  $C_5^*$  and  $C_{11}^*$   
139 coefficients, associated with the force, transmitted from *lu*-muscle. One possible explanation of  
140 these differences may be an imperfection of *lu*-muscle representation, which is the small muscle  
141 with a wide range of origin variation (Goldberg, 1970).

### 142 **Sensitivity analysis**

143           We studied how much the model-describing coefficients are sensitive to muscle force  
144 values. It appears that great differences can be observed for  $C_3^*$ ,  $C_4^*$ , and  $C_5^*$ . As a conclusion,  
145 the coefficients given by Chao *et al.* (1989) and used in most finger models could be inexact in  
146 some range of muscle forces. These results show how the force sharing among the EM bands  
147 changes if the force sharing among the muscles also changes. These findings could be important  
148 for accurate finger biomechanical modeling. This study should be distinguished from that of  
149 previous authors (Hurlbut and Adams, 1995; Wook *et al.*, 2008) that showed that the force  
150 distribution among the EM tendons does not depend on the overall muscle force level when the  
151 force distribution among the muscles remained constant.

### 152 **Perspectives**

153           The proposed model could be a tool to simulate the EM deformation during finger  
154 flexion-extension and change in force distribution. It may be directly incorporated into finger  
155 model or used to recalculate the coefficients for any physiological finger posture, muscle force  
156 level, and bone geometry. Moreover, it could improve the precision of the existing  
157 biomechanical finger models that represent the EM by equations (4) with coefficients determined

158 by optimization for required posture (Sancho-Bru *et al.*, 2001; Vigouroux *et al.*, 2007).  
159 Furthermore, more complex models, representing the EM as a membrane instead of the set of the  
160 elastic bands may be created. Moreover, the current model uses several assumptions, which can  
161 be subsequently removed as limiting the model accuracy. These assumptions concern:

- 162 1. *Bones*. The friction between the EM and the surface was not taken into account. The  
163 bones were modeled as cylinders with spheres at the ends. However, the joint surface  
164 of finger bones is irregular, which results in increase of the digit skeleton length with  
165 flexion. Zancolli (1979) reported a 20mm difference in finger skeleton length  
166 between full flexion and full extension postures. To minimize the influence of this  
167 effect the radius of the spheres were chosen as the mean radius of joint surfaces,  
168 which reduces the mean error among all postures.
- 169 2. *Muscles*. The muscle forces were represented by the vectors directed to the center of  
170 the muscle body. In the case of the extrinsic *ed*-muscle, the force vector was directed  
171 along the long extensor tendon. To increase the model precision the muscle body shift  
172 during the flexion should be taken into account. This is particularly true for lumbrical  
173 muscles, which shift distally during the finger flexion movement and change the  
174 orientation of the force.
- 175 3. *Tendons*. The tendons were modeled as springs with a linear elasticity model. This  
176 assumption conforms to experimental data. Garcia-Elias *et al* (1991) showed that the  
177 extensor mechanism tendons demonstrate a behavior, close to a liner elasticity model,  
178 in a physiological force range.

#### 179 **CONFLICT OF INTEREST**

180 The authors of this manuscript declare that there are no conflicts of interest

#### 181 **ACKNOWLEDGMENTS**

182 The authors thank Prof. François Moutet (CHU Grenoble), Dr. Lionel Reveret (INRIA  
183 Rhône-Alpes), and Dr. Isabelle Sivignon (GIPSA-Lab) for their valuable comments.

## REFERENCES

184

185 Chao, E.Y.S., An, K.-N., Cooney III, W.P., Linscheid, R.L., 1989. Biomechanics of the  
186 hand. A basic research study. World Scientific, Singapore.

187 Eyler, D.L., Markee, J.E., 1954. The anatomy and function of the intrinsic musculature of  
188 the fingers. *J. Bone Jt. Surg. - Am.* Vol. 36, 1–18.

189 Garcia-Elias, M., An, K.N., Berglund, L., Linscheid, R.L., Cooney, W.P., Chao, E.Y.S.,  
190 1991. Extensor mechanism of the fingers. I. A quantitative geometric study. *J. Hand Surg. Am.*  
191 16, 1130–1136.

192 Garcia-Elias, M., An, K.-N., Berglund, L.J., Linscheid, R.L., Cooney, W.P., Chao,  
193 E.Y.S., 1991. Extensor mechanism of the fingers. II. Tensile properties of components. *J. Hand*  
194 *Surg. Am.* 16, 1136–1140.

195 Giurintano, D.J., Sancho, J.L., 1999. Visualizing and Modeling the Extensor Hood  
196 Mechanism of the Fingers. *Am. Soc. Mech. Eng. Bioeng. Div.* 42, 551–552.

197 Goldberg, S., 1970. The Origin of the Lumbrical Muscles in the Hand of the South  
198 African Native. *Hand* 2, 168–171.

199 Harris, C., Rutledge, G.L., 1972. The functional anatomy of the extensor mechanism of  
200 the finger. *J. Bone Joint Surg. Am.* 54, 713–726.

201 Hu, D., Ren, L., Howard, D., Zong, C., 2014. Biomechanical Analysis of Force  
202 Distribution in Human Finger Extensor Mechanisms. *Biomed Res. Int.* 2014

203 Hurlbut, P.T., Adams, B.D., 1995. Analysis of finger extensor mechanism strains. *J.*  
204 *Hand Surg. Am.* 20, 832–840.

205 Leijnse, J.N.A.L., Quesada, P.M., Spoor, C.W., 2010. Kinematic evaluation of the  
206 finger's interphalangeal joints coupling mechanism — variability, flexion – extension  
207 differences, triggers, locking swanneck deformities, anthropometric correlations. *J. Biomech.* 43,  
208 2381–2393.

209           Leijnse, J.N. A L., Spoor, C.W., 2012. Reverse engineering finger extensor apparatus  
210 morphology from measured coupled interphalangeal joint angle trajectories - a generic 2D  
211 kinematic model. *J. Biomech.* 45, 569–578.

212           Qian, K., Traylor, K., Lee, S.W., Ellis, B., Weiss, J., Kamper, D., 2014. Mechanical  
213 properties vary for different regions of the finger extensor apparatus. *J. Biomech.* 47, 3094–  
214 3099.

215           Sachdeva, P., Sueda, S., Bradley, S., Fain, M., Pai, D.K., 2015. Biomechanical simulation  
216 and control of hands and tendinous systems. *ACM Trans. Graph.* 34.

217           Sancho-Bru, J.L., Perez-Gonzalez, A., Vergara-Monedero, M., Giurintano, D., 2001. A 3-  
218 D dynamic model of human finger for studying free movements. *J Biomech* 34, 1491–1500.

219           Schultz, R., Furlong II, J., Storace, A., 1981. Detailed anatomy of the extensor  
220 mechanism at the proximal aspect of the finger. *J. Hand Surg. Am.* 6, 493–498.

221           Schweitzer, T.P., Rayan, G.M., 2004. The terminal tendon of the digital extensor  
222 mechanism: Part I, anatomic study. *J. Hand Surg. Am.* 29, 903–908.

223           Shrewsbury, M.M., Johnson, R.K., 1977. A systematic study of the oblique retinacular  
224 ligament of the human finger: its structure and function. *J. Hand Surg. Am.* 2, 194–199.

225           Valero-Cuevas, F.J., Lipson, H., 2004. A computational environment to simulate  
226 complex tendinous topologies. *Conf. Proc. IEEE Eng. Med. Biol. Soc.* 6, 4653–4656.

227           Vaz, A., Singh, K., Dauphin-Tanguy, G., 2015. Bond graph model of extensor  
228 mechanism of finger based on hook–string mechanism. *Mech. Mach. Theory* 91, 187–208.

229           Vigouroux, L., Quaine, F., Labarre-Vila, A., Amarantini, D., Moutet, F., 2007. Using  
230 EMG data to constrain optimization procedure improves finger tendon tension estimations  
231 during static fingertip force production. *J. Biomech.* 40, 2846–2856.

232           Wook, S., Chen, H., Towles, J.D., Kamper, D.G., 2008. Estimation of the effective static  
233 moment arms of the tendons in the index finger extensor mechanism 41, 1567–1573.

234 Zancolli, E., 1979. Structural and Dynamic Bases of Hand Surgery. J.B. Lippincott  
235 Company, Philadelphia; Toronto.

Fig. 1a – the simplified anatomic view of the extensor mechanism of the left hand long finger (dorsal view). 1b – lateral view. The muscles (blue), tendons (green), and ligaments (light blue) are shown. 1c – the schematic view of the proposed model. The structures included in the model are denoted by numbers from 1 to 10 and listed in Table 1. For pair bands, located at both ulnar and radial side, only radial bands are enumerated.

Fig. 2. The experimentally defined coefficients  $\hat{C}_q$  from the equations (4) shown in comparison with the corresponding model-characterizing coefficients  $C_q^*$ . The former values are depicted by filed bars, the latter values are depicted by the hatched bars.

Fig. 3. The extensor mechanism simulation results during three finger postures. Left to right:(a) full flexion [DIP = 90°; PIP = 90°; MCP = 90°], (b) mid-flexion [DIP = 30°; PIP = 45°; MCP = 45°], (c) full extension [DIP = 0°; PIP = 0°; MCP = 0°]; the scaled-up retinacular and triangular ligaments during full flexion (d) and full extension (e).

Fig. 4. The sensitivity index  $SI$ , showing the sensitivity of model-characterizing coefficients  $C_q^*$  to variation of muscle force values.

Figure 1  
[Click here to download high resolution image](#)

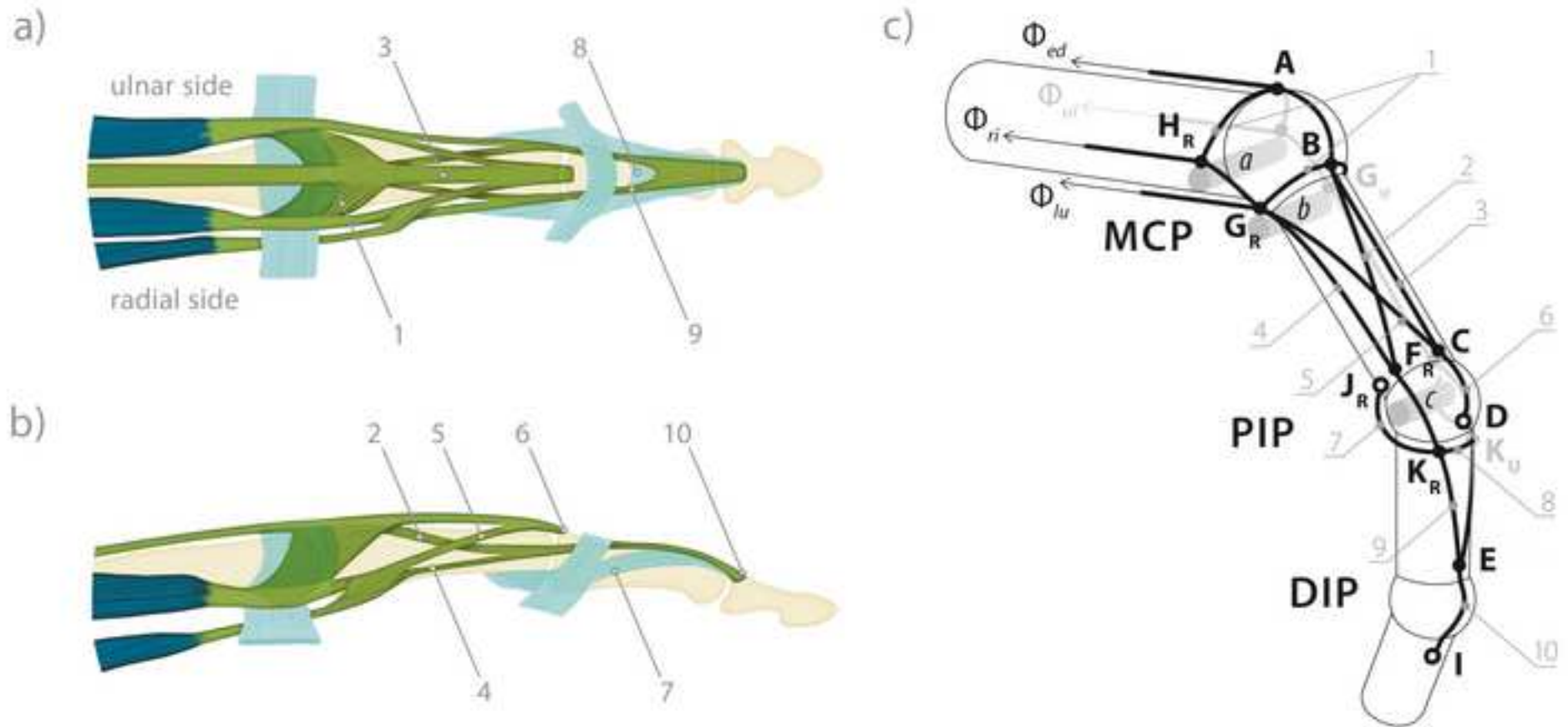
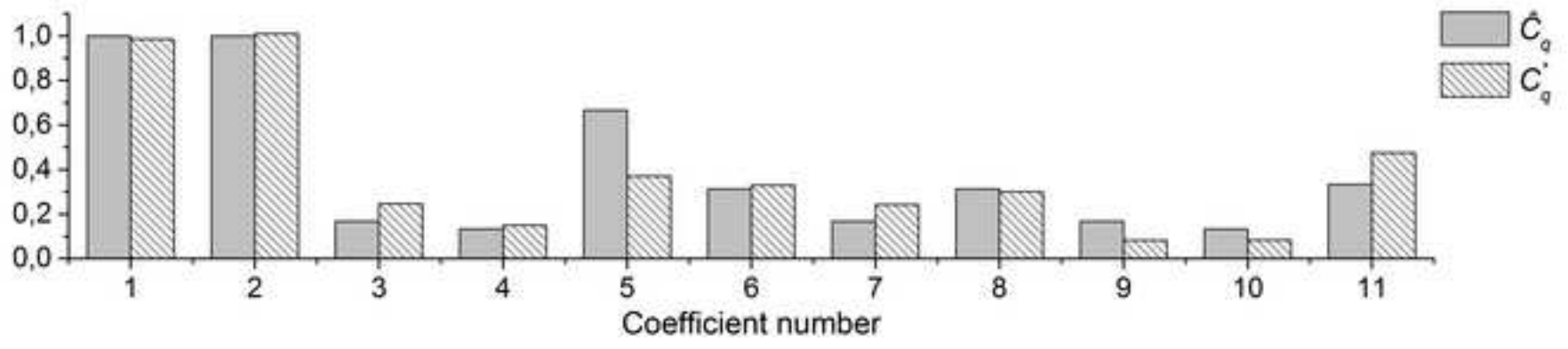


Figure 2  
[Click here to download high resolution image](#)



**Figure 3**  
[Click here to download high resolution image](#)

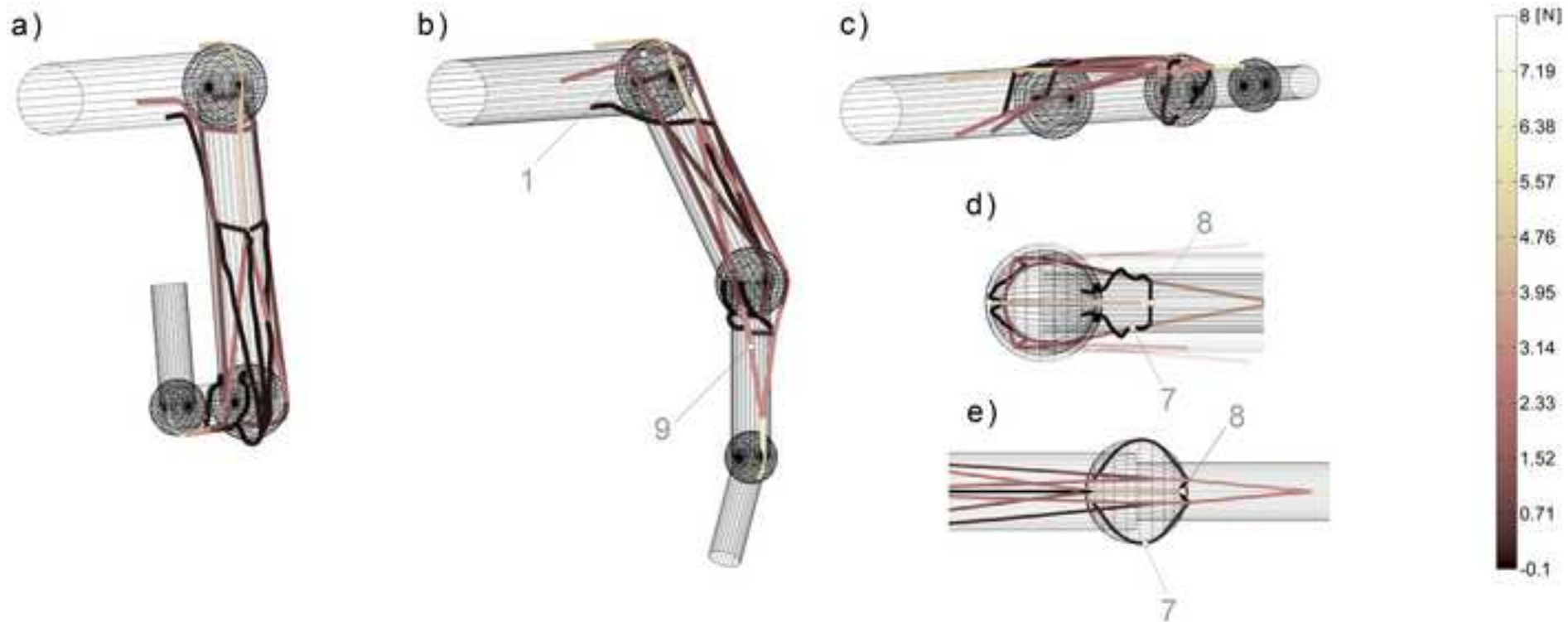
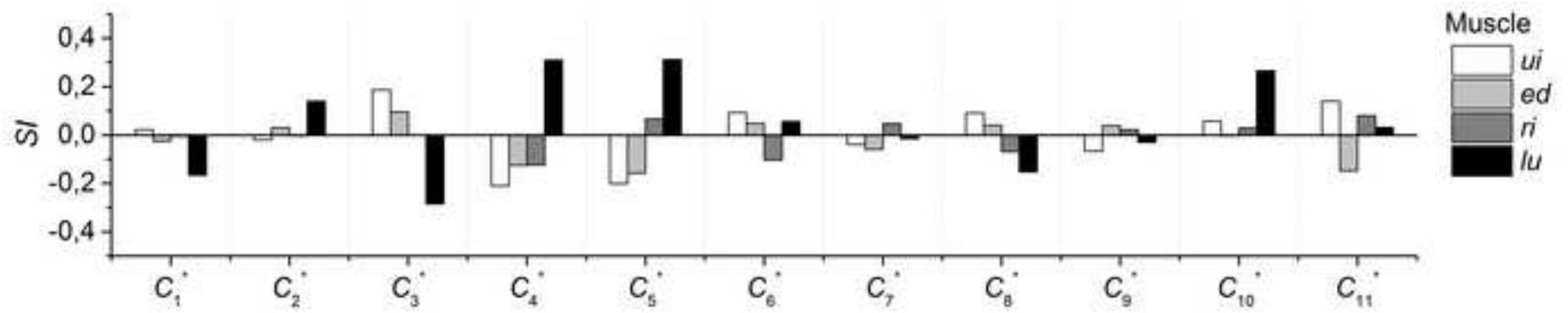


Figure 4  
[Click here to download high resolution image](#)



**Table 1. The elements of the extensor mechanism, included into the model**

Element number	Extensor mechanism element name	Abbreviation	Length (mm)	Thickness (mm)	Modulus of elasticity (MPa)
1	Proximal interosseous hood, radial and ulnar	-	18.4±2.5 <sup>a</sup>	1.19±0.33 <sup>c</sup>	64.87±29.30 <sup>c</sup>
	Distal interosseous hood, radial and ulnar	-	18.5±3.0 <sup>a</sup>		
2	Extensor lateral band, radial and ulnar	<i>el</i>	N/A	N/A	N/A
3	Extensor medial band	-	33.6±4.4 <sup>a</sup>	1.38±0.29 <sup>c</sup>	114.03±61.34 <sup>c</sup>
4	Interosseous lateral band, radial and ulnar	-	37.1±2.6 <sup>a</sup>	N/A	N/A
5	Interosseous medial band, radial and ulnar	<i>im</i>	36.2±1.9 <sup>a</sup>	N/A	N/A
6	Medial extensor tendon	<i>me</i>	11.2±1.8 <sup>a</sup>	1.20±0.31 <sup>c</sup>	125.31±62.06 <sup>c</sup>
7	Oblique retinacular ligament, radial and ulnar	-	15 <sup>d</sup>	N/A	N/A
8	Triangular ligament	-	5.4±1.1 <sup>b</sup>	N/A	N/A
9	Lateral band, radial and ulnar	<i>rb</i> and <i>ub</i>	18.4±4.3 <sup>a</sup>	1.20±0.39 <sup>c</sup>	157.02±138.37 <sup>c</sup>
10	Terminal extensor tendon	<i>te</i>	10.1±2.6 <sup>b</sup>	1.07±0.20 <sup>c</sup>	96.97±51.29 <sup>c</sup>

<sup>a</sup>(Garcia-Elias et al., 1991);

<sup>b</sup>(Schweitzer and Rayan, 2004);

<sup>c</sup>(Qian et al., 2014);

<sup>d</sup>(Shrewsbury and Johnson, 1977);

N/A denotes non-available data

**Table 1. The parametrization results**

Length of extensor lateral band $l_{el}$ (mm)	38.0
Length of interosseous medial band $l_{im}$ (mm)	32.7
Cost-function $J$	0.11

**Supplementary Material**

[Click here to download Supplementary Material: Table 3.docx](#)